A hidden demethylation pathway removes mercury from rice plants and mitigates mercury flux to food chains

Wenli Tang[1#], Xu Bai[2,3#], Yang Zhou[1#], Christian Sonne[4*], Mengjie Wu[1], Su Shiung Lam[5], Holger Hintelmann[6], Carl P.J. Mitchell[7], Alexander Johs[8], Baohua Gu[8], Luís Nunes[9], Cun Liu[10], Naixian Feng[11], Sihai Yang[12], Jörg Rinklebe[13,14], Yan Lin[15], Long Chen[16], Yanxu Zhang[17], Yanan Yang[1], Jiaqi Wang[1], Shouying Li[1], Qingru Wu[18], Yong Sik Ok[19], Diandou Xu[2], Hong Li[2], Xu-Xiang Zhang[1], Hongqiang Ren[1], Guibin Jiang[20], Zhifang Chai[2], Yuxi Gao[2*], Jiating Zhao[2,21*], Huan Zhong[1*]

[1] School of the Environment, Nanjing University, State Key Laboratory of Pollution Control and Resource Reuse, Nanjing 210023, China. [2] Key Laboratory for Biomedical Effects of Nanomaterials and Nanosafety, Institute of High Energy Physics (IHEP), Chinese Academy of Sciences (CAS), Beijing 100049, China. [3] University of Chinese Academy of Sciences, Beijing 100049, China. [4] Department of Bioscience, Arctic Research Centre, Aarhus University, Roskilde, Denmark. [5] Higher Institution Centre of Excellence (HICoE), Institute of Tropical Aquaculture and Fisheries (AKUATROP), Universiti Malaysia Terengganu, Kuala Nerus, Terengganu 21030, Malaysia. [6] Department of Chemistry, Trent University, Peterborough, Ontario K9L 0G2, Canada. [7] Department of Physical and Environmental Sciences, University of Toronto Scarborough, 1265 Military Trail, Scarborough, Ontario M1C 1A4, Canada. [8] Environmental Sciences Division, Oak Ridge National Laboratory, Oak Ridge, Tennessee 37830, United States. [9] Faculty of Sciences and Technology, Civil Engineering Research and Innovation for Sustainability Center, University of Algarve, Faro, Portugal. [10] Key Laboratory of Soil Environment and Pollution Remediation, Institute of Soil Science, Chinese Academy of Sciences, Nanjing 210008, China. [11] College of Life Science and Technology, Jinan University, Guangzhou 510632, China. [12] State Key Laboratory of Pharmaceutical Biotechnology, School of Life Sciences, Nanjing University, 210023 Nanjing, China. [13] University of Wuppertal, School of Architecture and Civil Engineering, Institute of Foundation Engineering, Water and Waste Management, Laboratory of Soil and Groundwater Management, Pauluskirchstraße 7, 42285 Wuppertal, Germany. [14] Department of Environment, Energy and Geoinformatics, Sejong University, 98 Gunja-Dong, Guangjin-Gu, Seoul, Republic of Korea. [15] Norwegian Institute for Water Research, Oslo, 0349, Norway. [16] Key Laboratory of Geographic Information Science (Ministry of Education), School of Geographic Sciences, East China Normal University, Shanghai 200241, China. [17] School of Atmospheric Sciences, Nanjing University, Nanjing, China. [18] State Key Joint Laboratory of Environmental Simulation and Pollution Control, School of Environment, Tsinghua University, Beijing 100084, China. [19] Korea Biochar Research Center, APRU Sustainable Waste Management Program and Division of Environmental Science and Ecological Engineering, Korea University, Seoul 02841, Republic of Korea. [20] State Key Laboratory of Environmental Chemistry and Ecotoxicology, Research Center for Eco-Environmental Sciences,

Chinese Academy of Sciences, 100085 Beijing, China. [21] Department of Environmental Science, Zhejiang University, Hangzhou 310058, China.

[#] These authors contributed equally to this work.

[*]Corresponding authors: Christian Sonne (cs@ecos.au.dk); Jiating Zhao (zhaojt@ihep.ac.cn); Yuxi Gao (gaoyx@ihep.ac.cn); Huan Zhong (zhonghuan@nju.edu.cn).

Abstract: Dietary exposure to methylmercury (MeHg) causes irreversible damage to human cognition, and is mitigated by photolysis and microbial demethylation of MeHg. Here, we report a hidden pathway of MeHg demethylation independent of light and microorganisms. This natural pathway exists in crops and is driven by reactive oxygen species generated *in vivo*, rapidly transforming MeHg to inorganic Hg and then eliminating Hg from plants as gaseous Hg^0. Methylmercury concentrations in rice grains would increase by 2.4- to 4.7-fold without this pathway, which equates to IQ losses of 0.01−0.51 points/newborn in major rice consuming countries, corresponding to annual economic losses of $30.7−84.2 billion USD globally. This newly discovered pathway effectively removes Hg from human food webs, playing an important role in exposure mitigation and global Hg cycling.

Keywords: Rice, Microbes, Demethylation, Health risks, Reactive oxygen species, Methylmercury

Global concerns over the potent neurotoxin methylmercury (MeHg) have persisted for decades. After entering the biosphere, MeHg is efficiently transferred along food chains, magnifying its concentration up to ten million-fold [1]. Even low-level dietary exposure to this ubiquitous toxin causes irreversible neurological damage in humans [2], reducing the intelligence quotient (IQ) of newborns [3] and their lifetime earnings. MeHg exposure has been reported to cause IQ decrements of 2,420,000, 600,000 and 264,000 points per year in China, European countries and the United States, respectively, corresponding to yearly economic losses of approximately $7.3, 11 and 5 billion USD [4–7]. Human exposure to MeHg is largely mitigated by its demethylation in natural environments, during which this potent neurotoxin is converted into less toxic inorganic forms prior to entering human food webs. Photolysis [8,9] and microbial demethylation [10–12] are the two widely recognized pathways of MeHg demethylation in the environment [13], effectively reducing the amount of MeHg available for bioaccumulation.

Despite decades of research and advances in understanding light- and microbe-mediated demethylation in surface water, soils and sediments [10,13–16], the role of plants in degrading MeHg remains unclear and is largely ignored. Although MeHg demethylation within rice has been inferred [17–19], it remains unknown what drives this process within plants which are key starting points for MeHg into human food webs. Particularly, rice (*Oryza sativa* L.) has been identified as a major dietary source of MeHg [20] and is responsible for up to 96% of the MeHg exposure in inland China [21]. More importantly, rice is the most common food ingredient in ready-to-eat formulas for infants, contributing approximately half of their MeHg exposure and putting them at greater risks compared with adults [22]. Deciphering the pathway of plant-mediated demethylation is therefore critical to understanding how MeHg makes its way from soils to crops and then to humans. However, it is challenging to distinguish demethylation driven by plants themselves, rhizospheric/endophytic microorganisms and/or light, all of which are entangled in the complex soil-plant system [17,19]. Tackling this challenge requires tracing Hg transformations within plants and ruling out the contributions of both microbial demethylation and photolysis [19], by using multidisciplinary tools and providing multiple lines of evidence.

Demethylation occurs within crops

Here, we explore MeHg demethylation within rice plants using an enriched Hg isotope tracer approach. During the cultivation of rice seedlings in a non-Hg spiked nutrient solution after exposure to dissolved $Me^{202}Hg$ (Fig. 1a), we observe mass decreases in either $Me^{202}Hg$ or ambient MeHg (naturally occurring MeHg, further discussed in Supplementary Text 1) in rice tissues (Fig. 1b, c and Extended Data Fig. 1a−c), reflecting that MeHg demethylation occurs within plants. Meanwhile, the accumulation of inorganic ^{202}Hg ($I^{202}Hg$, calculated as the difference between total ^{202}Hg and $Me^{202}Hg$, Fig. 1b, c) is also observed during the cultivation, providing evidence that decreases in $Me^{202}Hg$ are due to the transformation of $Me^{202}Hg$ to $I^{202}Hg$. The $I^{202}Hg$ observed in rice plants is not derived from the uptake of $I^{202}Hg$ by roots since it is undetectable in the exposure medium or root washing solutions (Fig. 1d and Extended Data Fig. 2). Conversely, Hg methylation within plants is not supported by our data since no $Me^{200}Hg$ is detected in rice tissues after exposure to dissolved $I^{200}Hg$ (Extended Data Fig. 1d−e and Supplementary Text 2).

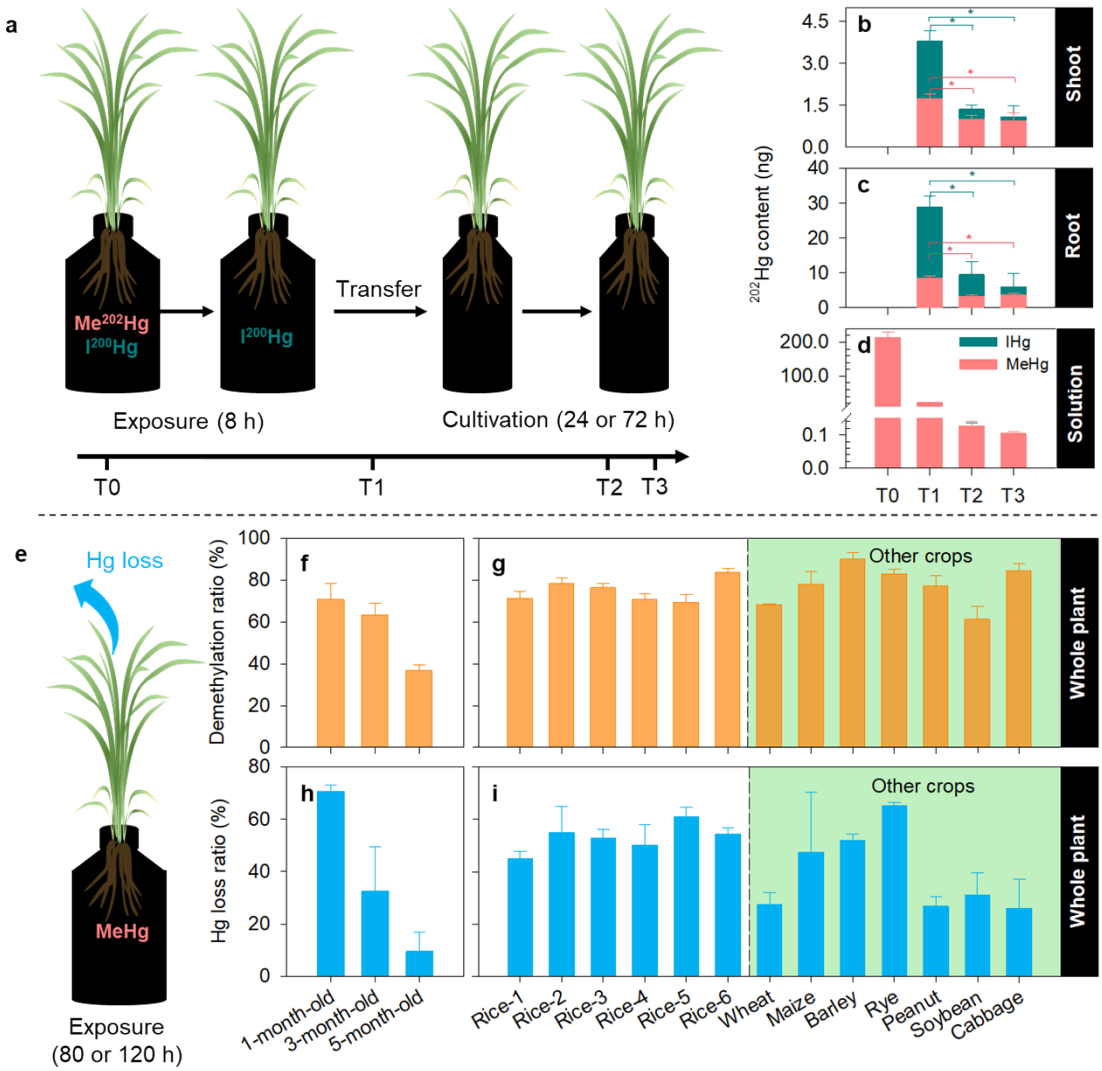

Fig. 1 | Evidence of MeHg demethylation *in vivo* and Hg release from crops. (a) experimental setup and (b–d) the mass of ^{202}Hg in plant tissues and exposure/cultivation solutions in the enriched isotope experiment; (e) experimental design, (f and h) MeHg demethylation ratios and (g and i) Hg loss ratios in rice growth stage experiment and crop experiment. T0 refers to the time when exposure started (with $Me^{202}Hg$ and $I^{200}Hg$ spiked into solutions); T1 refers to the time when exposure ended and plants were transferred (only significant proportion of $I^{200}Hg$ remained in the solution, Supplementary Text 3); T2 and T3 refer to times when plants were further cultivated in Hg-free solution for 24 h (T2) and 72 h (T3), respectively. Demethylation ratio is defined as the proportion of demethylated MeHg to total MeHg absorbed by plants; total adsorbed MeHg is calculated by subtracting MeHg contents remained in the solution after exposure and in root washing solutions from the total MeHg content in the solution before exposure; demethylated MeHg is calculated by subtracting MeHg contents detected in plants and in shoot washing solutions from total absorbed MeHg. Hg loss ratio is defined as the ratio of the content of lost THg to total THg absorbed by plants from roots; total absorbed THg is calculated by subtracting the THg content remained in solution after exposure and in root washing solutions from the total THg content in

solution before exposure; lost Hg is calculated by subtracting THg contents detected in plants and in shoot washing solutions from total absorbed THg. The contents of THg and MeHg are calculated as a total mass (ng), with the effect of variability in biomass excluded. Rice-1 was used in the enriched isotope and the rice growth stage experiments. Asterisk (*) indicates significant ($p < 0.05$) differences between two time points. All values are presented as mean ± SD, n = 3. Some error bars may be too small to be visible in graphs.

The demethylation of MeHg occurs within rice plants at all growth stages (showing a demethylation ratio of 37−71%, particularly at the early stages, Fig. 1f), and the demethylation ratios are consistently high in five other varieties of rice and in seven other major crop species (61−90%, Fig. 1g). Moreover, our data also support that MeHg demethylation occurs predominantly in roots, as a higher proportion of IHg is found in roots than that in shoots following MeHg exposure (30−95% in roots versus 10−63% in shoots, Supplementary Text 4). In addition, demethylation occurs regardless of MeHg exposure concentrations (0−100 μg/L) or the presence of soil pore water (Extended Data Fig. 3 and Supplementary Text 5), supporting the representativeness of these experimental findings to natural environments.

In addition to the transformation of MeHg into IHg within plants, we report the subsequent reduction and release of Hg into the air following demethylation. The mass of total isotopic Hg in rice tissues (THg, for either ^{202}Hg or ^{200}Hg) decreases significantly during the course of the enriched isotope experiment (Fig. 1b−c and Extended Data Fig. 1d−e). Similarly, Hg loss from plants during MeHg exposure is also observed at different growth stages of rice, in different rice varieties and other crop plants, with loss ratios of 10−70%, 45−61% and 26−65%, respectively (Fig. 1h and i). By carrying out the Hg-release experiment in a closed system (Extended Data Fig. 4), we detect only Hg^0 and no other Hg species in the surrounding air after exposing rice plants to dissolved MeHg, with the amount of released Hg^0 being 1.8 times higher than that from plants exposed to the non-spiked solution. The released Hg^0 does not originate from the exposure solution nor from roots, considering that THg and MeHg concentrations are comparable in exposure medium and tissue washing solutions (Extended Data Figs. 2 and 5) and thus the content of dissolved Hg^0 is extremely low. Instead, the released gaseous Hg^0 is derived from the *in vivo* transformation of the absorbed MeHg. By spiking Me^{199}Hg into the exposure solution, we find a significant

amount of $^{199}Hg^0$ (3.6 ng, details in Supplementary Text 6) is captured from the ambient air. This provides direct evidence that rice plants could release Hg^0 to the ambient air after MeHg absorption and its *in vivo* transformation.

The exchange of Hg between soil and air is a key process in global Hg cycling, whereas how plants channel Hg flux to the air is unclear [23]. Our results decipher this process by revealing that a sequence of MeHg uptake-MeHg demethylation-IHg reduction by plants is an efficient pathway of soil-air Hg exchange, during which Hg is *in vivo* transformed from the most bioavailable and neurotoxic species (i.e., MeHg) into less bioavailable and less toxic species (i.e., IHg and Hg^0) [24]. We further estimate that Hg release from rice plants via this process is ~30-fold (ranging 2−2,907 fold) greater than that via IHg uptake-IHg reduction (calculated using the Hg release capacities obtained from the enriched isotope experiment and the documented MeHg to IHg ratios in pore water, details in Methods, Section 4). The relatively large uncertainty range is mainly attributed to variations in the reported MeHg to IHg ratios (Supplementary Table 8). However, further studies are warranted to assess the amount of Hg release via the process (i.e., MeHg uptake-MeHg demethylation-IHg reduction by plants), especially in the field, as well as the relative importance of this pathway and the direct Hg emission from soils, a well-recognized pathway of soil-air Hg flux [25–27].

Singlet oxygen induces the demethylation

To elucidate the pathway of MeHg demethylation within plants, we examine the potential involvement of microbial degradation and photolysis, the two most commonly recognized demethylation pathways [10–12]. We demonstrate that MeHg demethylation occurs irrespective of the presence of microorganisms. This is evidenced by the significant demethylation in microbe-excluded supernatant of root homogenate (40%, < 0.22 μm), in microbe-inhibited root homogenates (54% under antibiotics addition and 64−66% under alkaline conditions where most microorganisms can't survive) and in axenically cultured rice plants (38%) and rice callus (38%) (Fig. 2a−c). These moderate differences in demethylation ratios between normal and axenic rice plants/callus are not attributed to microorganisms but to the differences in cultivation and exposure conditions (Supplementary Text 7). Additionally, the minor role of microorganisms in demethylation is further supported by the incapability of demethylation by root-isolated (Fig. 2d) or rhizospheric microorganisms (Extended Data Figs. 2 and 5), higher

demethylation under aerobic conditions than anaerobic ones (Fig. 2a, Supplementary Text 7), as well as the slower rate of demethylation documented for microorganisms (e.g., half-life > 1 d in sediments) [14] compared to rice plants (half-life ~2 h, Fig. 2e). Meanwhile, MeHg demethylation within plants is light-independent. This is due to the minor effect of light on MeHg demethylation both in living plants and in root homogenates (Extended Data Fig. 6), and most MeHg is demethylated in roots where light is absent (Fig. 1b and c, and Supplementary Text 4).

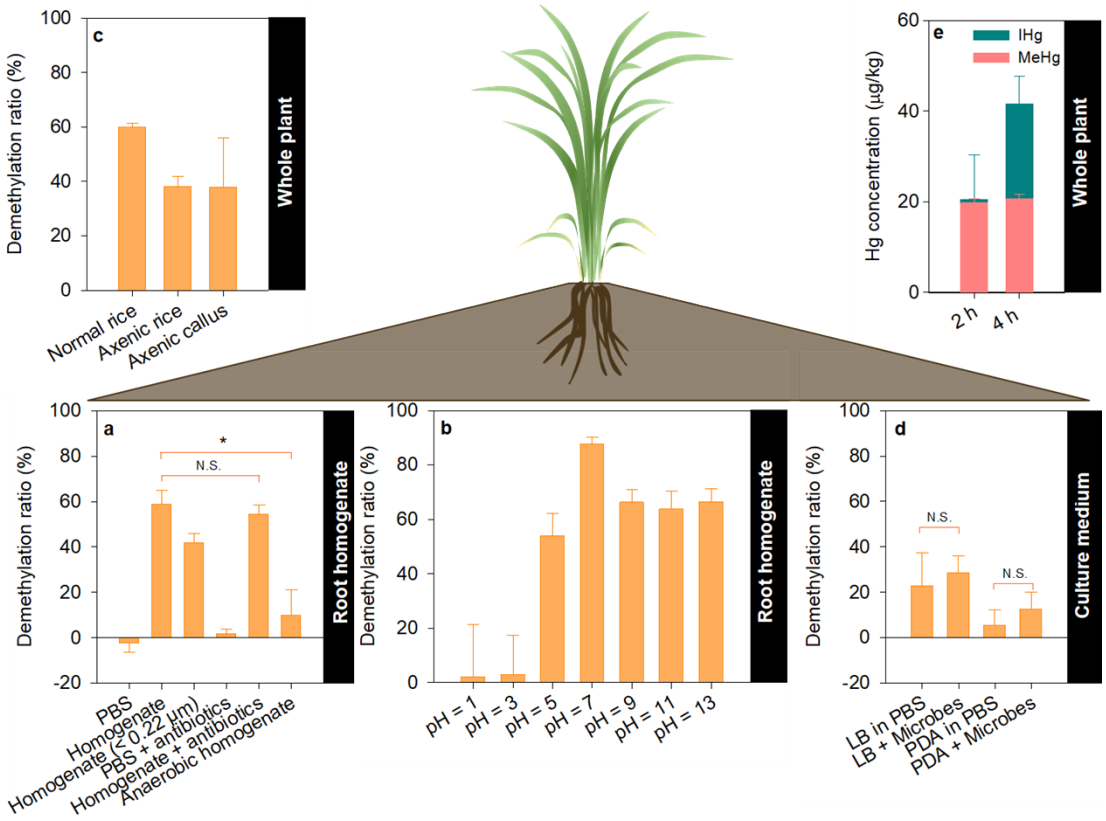

Fig. 2 | Lines of evidence demonstrating *in vivo* MeHg demethylation irrespective of microorganisms. MeHg demethylation ratios in (a) homogenates with microbes excluded or inhibited, (b) homogenates under different pH, (c) normal and axenically cultured rice plants/callus (2-week-old), (d) media with/without isolated microorganisms and (e) Hg concentrations in whole rice plant after being exposed to dissolved MeHg for 2 and 4 h. PBS refers to phosphate buffer (Na/K, 20 mM, pH = 7.0), and LB and PDA represent the Luria Bertani and potato dextrose agar media for bacteria and fungi, respectively. In (a), PBS and PBS + antibiotics were set as control groups; the treatment of Anaerobic homogenate means roots were homogenized and incubated both under anaerobic conditions. In (c), normal rice refers to rice seedlings cultivated in an environmental chamber, and axenic rice and callus indicate those cultivated in a sterilized environment. In (e), the presented Hg concentrations are the differences between the Hg concentrations in plants exposed to dissolved MeHg and those in plants exposed to non-spiked $CaCl_2$ solution. Both normal rice and

axenically cultivated rice in panel (c) were 2-week-old. N.S. indicates no significant differences ($p > 0.05$) between two treatments. Data are presented as mean ± SD, n = 3.

Our analyses of reactive oxygen species (ROS) demonstrate that *in vivo* generated singlet oxygen is responsible for the observed demethylation within rice plants, being the mechanism of this light- and microbe-independent demethylation pathway. It has been reported that ROS such as singlet oxygen, hydroxyl radical and superoxide anion could induce the photolysis of MeHg in surface water [28,29]. However, ROS-mediated MeHg demethylation within organisms has been largely ignored, particularly for plants, though those ROS are commonly found in plant cell organelles including mitochondria, chloroplast and nucleus and irrespective of light [30,31]. Here, we provide multiple lines of evidence that support the light- and microbe-independent demethylation of MeHg in plants driven by singlet oxygen. Firstly, the additions of selective quenchers to the root homogenate inhibit MeHg demethylation by > 70% only in the singlet oxygen-quenched treatments during the whole growth period of rice plants (Fig. 3a and Extended Data Fig. 7a). Secondly, we measure singlet oxygen in living plants using singlet oxygen sensor green (SOSG, Fig. 3b and Extended Data Fig. 7b), and in fresh root tissue (Fig, 3c) and supernatant of root homogenate (< 0.22 μm, Extended Data Fig. 8a) using electron paramagnetic resonance (EPR). At all growth stages, the signal of singlet oxygen is observed in rice plants, especially in roots (Fig. 3b and Extended Data Fig. 7b). It should be noted that the singlet oxygen detected in plants is not induced by homogenization or light irradiation (Extended Data Fig. 8 and Supplementary Text 8). Thirdly, demethylation under singlet oxygen attack is further supported by results of density-functional theory calculations (Extended Data Fig. 9 and Supplementary Text 9) and the DRs quantified in singlet oxygen-generating system (Extended Data Fig. 10). We thus propose that the complexation of MeHg with thiols, which are abundant in plants, could lower the activation barrier to break the Hg-C bond of MeHg, facilitating the electrophilic attack of the Hg-C bond by singlet oxygen (Supplementary Text 9). Considering that singlet oxygen commonly exists across microorganisms, plants and animals [32,33], more work is necessary to explore the importance of this hidden demethylation pathway in other taxa.

This *in vivo* demethylation mechanism differs fundamentally from previously reported ROS-mediated MeHg photolysis in surface water [28] and at the soil-water interface [34], considering that plant demethylation is light-independent. Although ROS

or non-oxygen-centered radical-induced MeHg demethylation in animals has been hypothesized in a few earlier studies [35–37], the ROS or radicals were generated by adding exogenous oxides or activators *in vitro*, while the *in vivo* generated ROS were not determined and their roles in MeHg demethylation were unknown in those studies. Additionally, the role of light or microorganisms in the observed MeHg demethylation of those previous studies was not excluded. Photolysis and microbial demethylation are commonly recognized as the dominant pathways that degrade MeHg in the ambient environment. The discovery of this light- and microbe-independent pathway expands beyond the boundaries of knowledge on MeHg degradation in the nature, extending MeHg demethylation research from the ambient environment to flora and elucidating Hg transformation upon the initiation of bioaccumulation at the bottom of food webs.

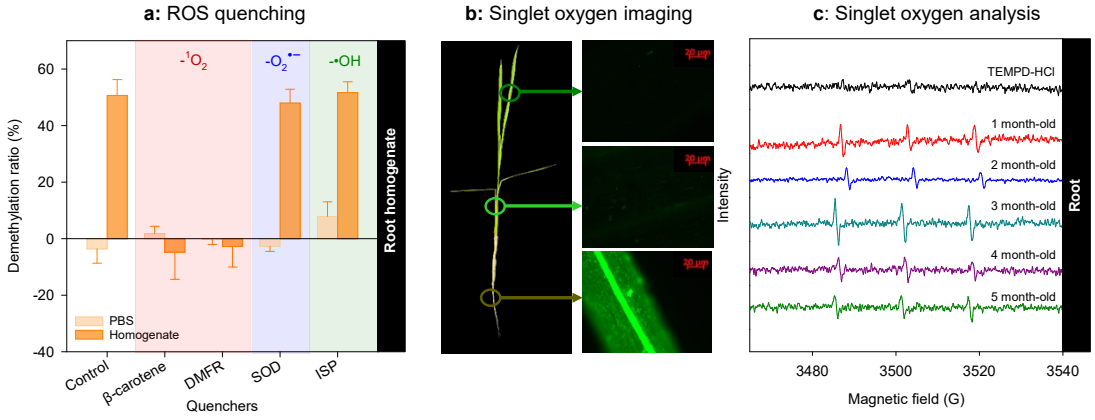

Fig. 3 | Lines of evidence showing the dominant role of singlet oxygen in MeHg demethylation in rice plants. (a) the response of MeHg demethylation in root homogenates to radical quencher additions, (b) the appearance of singlet oxygen in different tissues using SOSG and (c) the signal of singlet oxygen from rice roots using EPR. In (a), β-carotene (10 mM) and dimethylfuran (DMFR, 50 mM) are quenchers of singlet oxygen; superoxide dismutase (SOD, 0.5 mg/L) is a quencher of the superoxide anion ($O_2^{\bullet-}$); isopropyl alcohol (ISP, 50 mM) is a quencher of the hydroxyl radical (•OH). In this experiment, demethylation ratio is defined as the proportion of demethylated MeHg to total spiked MeHg, where the demethylated MeHg (μg/L) is calculated by subtracting the remaining MeHg (μg/L) from total spiked MeHg (μg/L). Phosphate buffer (PBS, Na/K, 20 mM, pH = 7.0) was set as a control and the root homogenate was obtained by grinding rice roots in PBS (pH = 7.0) at a ratio of 1 g fresh tissue/10 mL PBS. Data are presented as the mean ± SD, n = 3. In (c), the black line indicates the EPR signal from 500 mM 2,2,6,6-tetramethyl-4-piperidone hydrochloride (TEMPD-HCl, dissolved in 20 mM PBS buffer/D_2O, pH = 7.0), while colored lines indicate the EPR signal from fresh roots at different growth stages (rice plants cultivated in 2 mL of 500 mM TEMPD-HCl dissolved in 20 mM PBS/D_2O).

Demethylation in rice mitigates exposure

We use a health risk model to assess the protective effects of MeHg demethylation within rice on human health. The cognitive deficit (ΔIQ) is chosen to show the health endpoints based on epidemiological studies that have shown a linear dose-response relationship between maternal intake of MeHg and fetal IQ decrements [38–40]. By developing a MeHg accumulation model and applying Monte Carlo simulation, we estimate the IQ decrements prevented by MeHg demethylation within rice in 159 countries/regions. Results demonstrate that MeHg demethylation within rice plants greatly reduces the concentrations of neurotoxic MeHg in rice grains, moderating IQ losses and providing economic benefits (Data S1). The results of the modeling analysis show that in the absence of MeHg demethylation within rice plants, MeHg levels in rice grains would increase by a factor of 2.4 (Scenario A, simulating the minimum MeHg demethylation within rice plants, see Materials and Methods, section 3) or 4.7 (Scenario B, simulating the maximum MeHg demethylation within rice plants), leading to increased human exposure to MeHg. For instance, in Indonesia, ranking 3rd in rice production and 4th in population in the world, the observed rice MeHg concentration averages at 4.6 μg/kg [41], while it would increase to 10.6 (Scenario A) or 21.1 (Scenario B) μg/kg without *in vivo* demethylation. Under the assumption that the average body weight of Indonesians is 60 kg, the estimated daily intake of MeHg from rice consumption would be 0.07 (Scenario A) or 0.13 (Scenario B) μg MeHg/kg body weight/d, comparable to or higher than the maximum acceptable oral dose suggested by the USEPA (0.1 μg MeHg/kg body weight/d). The reductions in rice MeHg levels resulting from demethylation within plants avoid IQ decrements by 0.01−0.19 (Scenario A, with a P90 of 0.03−0.44, Supplementary Table 1) or 0.03−0.51 points per fetus (Scenario B, with a P90 of 0.07−1.22, Supplementary Table 1) in regions with high rice consumption (> 100 g/capita/d, Fig. 4a). Taking the mainland of China for example, the prevented IQ decrements are 0.04−0.11 points/newborn, which are comparable to the total IQ decrements caused by dietary MeHg exposure in China (0.14 point) [7].

These modeled results clearly demonstrate the importance of MeHg demethylation within rice plants for protecting human health. Previous studies have shown that IQ deficits have direct and indirect effects on lifetime earnings [42,43]. Combining the coefficient of IQ to lifetime earnings, the prevented IQ decrement and the annual

number of new births in an area (see Materials and Methods, section 3), we estimate that the annual economic benefits generated as a result of MeHg demethylation within rice plants to be $30.7−84.2 billion USD globally. Among all the studied countries, China, Indonesia, India, the US and Japan are the top 5 countries benefiting the most from MeHg demethylation in rice plants (Fig. 4b), with average annual benefits of $15.8, 6.5, 1.3, 1.2 and 0.4 (Scenario A, with a P90 of 36.3 15.3, 2.2, 3.5, and 0.9, respectively, Supplementary Table 2) or $43.8, 17.2, 3.5, 3.3 and 1.2 (Scenario B, with a P90 of 101.0, 40.8, 6.1, 9.5, and 2.6, respectively, Supplementary Table 2) billion USD. Indeed, these benefits may even surpass those from controlling Hg emissions, the primary ongoing global strategy for mitigating MeHg risks. For instance, in China, the predicted economic benefits provided by MeHg demethylation in rice are $15.8 (Scenario A) or 43.8 (Scenario B) billion dollars which are appreciably higher than the $8.4−21.6 billion dollars associated with the Hg emission control processes used in coal-fired power plants each year [44].

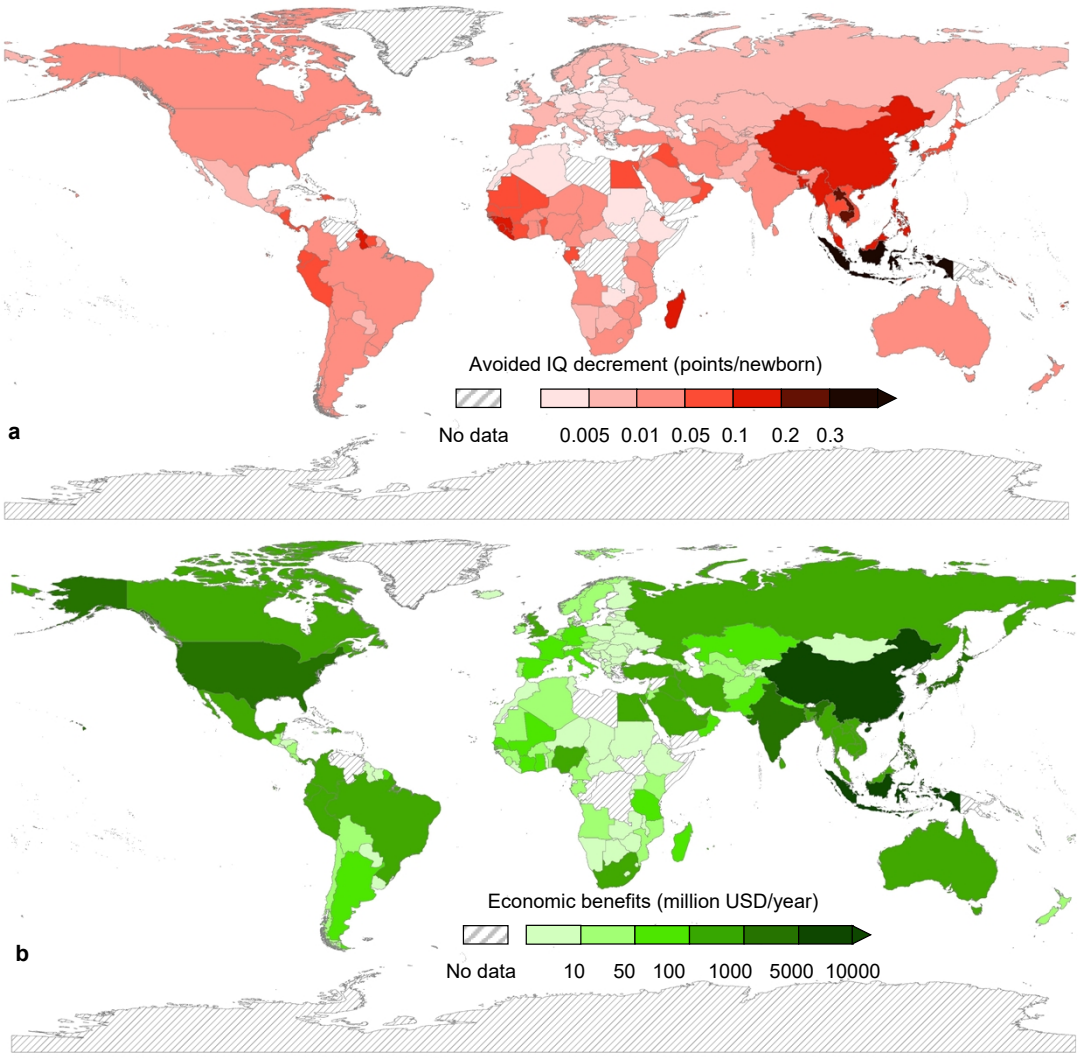

Fig. 4 | Prevented IQ decrement (a) and the associated economic benefit (b) resulting from MeHg demethylation by rice plants. Only the data in Scenario B are depicted here. More information can be found in Supplementary Tables 1−2 and Data S1 (including all the related parameters for the calculations of IQ decrement and economic benefit). The global map is provided by Natural Earth (https://www.naturalearthdata.com/downloads/10m-cultural-vectors/, accessed on 18 October 2022).

Our study reveals that plants act as a "channel" of Hg flux from the pedosphere to the atmosphere through efficient MeHg uptake by roots from the soil, rapid transformation *in vivo* irrespective of light/microbes and then the release of Hg^0 to the air. As a result, Hg is effectively removed from plants and re-directed to the air, and the observed MeHg bioaccumulation thus represents only a small proportion of MeHg absorbed by plants. Our results demonstrate that plants provide a highly beneficial ecosystem service by degrading MeHg *in vivo* thereby mitigating Hg flux to food chains. These findings call for rethinking the roles of plants in global Hg cycling. Further

studies should quantify Hg^0 release following *in vivo* demethylation in other systems such as forest and ocean, which would improve the mapping of global Hg cycling. We also call immediate attention from scientific communities to the future changes in the effectiveness of this natural barrier against MeHg accumulation in crop plants, e.g., under climate change which would impact plant physiology and ROS generation [45] and thus the global food security.

Materials and Methods

1. Experimental designs

Enriched isotope experiment. MeHg demethylation within rice plants was examined by applying the enriched isotope tracing technique. Briefly, rice seedlings (Wufeng, referred to as Rice-1) were cultivated hydroponically for one month in a climate-controlled plant growth chamber (25 °C, 14 h:10 h light: dark, the same for all exposure). A total of 45 seedlings with similar heights were selected and exposed to 0.01 M $CaCl_2$ solution spiked with ~0.4 μg/L $Me^{202}Hg$ (as $CH_3{}^{202}HgCl$, 97.7%) and ~0.15 μg/L $I^{200}Hg$ (as $^{200}Hg(NO_3)_2$, 79.7%). These Hg contents were chosen according to the reported values in paddy pore water [46] and MeHg/THg ratios in the pore water of wetlands and sediments (Supplementary Table 8), considering that data on MeHg in paddy pore water and MeHg/THg ratios are limited. The time when exposure started was defined as T0. $CaCl_2$ solution instead of soil pore water was used to exclude the effects of soil dissolved organic matter on MeHg uptake by plants and plant growth (Supplementary Text 5). After 8 h of exposure (T1), 15 seedlings were selected randomly and subjected to isotopic Hg analyses. The remaining 30 seedlings were transferred to 6 bottles, and each bottle contained 5 seedlings and 100 mL of nutrient solution (Hg free). These 6 bottles were placed in the growth chamber for further cultivation for 24 h (T2) or 72 h (T3) to investigate the dynamic of MeHg demethylation. After cultivation, all seedlings were harvested and separated into shoots and roots. Then, the tissues were washed sequentially with 8 mM cysteine solution and deionized (DI) water, oven dried to constant weight (at 40 °C) and ground for Hg

analyses. The efficiency of the washing procedure to remove surface-adsorbed MeHg has been tested in a previous experiment [47]. All the liquids, including the media before and after uptake, cysteine and DI washing solutions (referred to as washing solutions) and nutrient solution were collected with weights recorded and then acidified using HCl before Hg isotope analyses.

Rice growth stage experiment. To explore the demethylation capacity of rice plants at different growth stages, rice plants (Rice-1) were cultivated hydroponically in a growth chamber for 1, 3 and 5 months and then exposed to a 0.8 μg/L MeHg solution (containing 0.01 M $CaCl_2$) at room temperature. After 80-h exposure, the plants were harvested, washed (shoots and roots separated) and dried as described above. Solutions were also collected with weights recorded. All the plant tissues and solutions were subjected to MeHg and THg analyses.

Crop experiment. Six varieties of rice plants and seven common crop plants were selected to quantify MeHg demethylation *in vivo*. These rice varieties (i.e., Wufeng, Liangyou900, Xiangliangyou900, Akitakomati, Yueguang and Jingliangyouhuazhan, referred to as Rice-1, Rice-2, Rice-3, Rice-4, Rice-5 and Rice-6, respectively) are commonly planted in China, and these crop plants, i.e., rice, wheat, maize, barley, rye, peanut, soybean and cabbage are common crops according to the planting area worldwide (based on the FAO database). After being cultivated hydroponically for one month, each variety was exposed to an 80−500 mL (depending on the biomass of each species) of 100 μg/L MeHg solution (containing 0.01 M $CaCl_2$, referred to as Exposure) or 0.01 M $CaCl_2$ (referred to as Control) for 5 days. A 5-day exposure period was used, considering that MeHg demethylation in rice plants occurs within hours to days according to the results of our preliminary experiments. A relatively high concentration of MeHg, i.e., 100 μg/L, instead of an environmentally relevant concentration was applied to minimize the interference of background Hg, also considering that MeHg demethylation occurs regardless of the exposure concentrations (Extended Data Fig. 3 and Supplementary Text 5). After exposure, all seedlings were harvested, washed (with shoots and roots separated) and dried as described above before THg and MeHg analyses. All liquids, including media before and after exposure, cysteine and DI

washing solutions, were collected with weights recorded and then acidified with HCl to measure Hg levels.

Demethylation-impacting factor experiments. To explore possible factors that may impact MeHg demethylation, we quantified demethylation ratios under different conditions both *in vivo* and *in vitro.* Specifically, the effects of light, microorganisms and exposure concentration/matrix/duration on MeHg demethylation *in vivo*, as well as the effects of light, pH and microorganisms on MeHg demethylation *in vitro*, were explored using Rice-1. Details of the experimental design are summarized in Supplementary Tables 3 and 4.

For *in vivo* tests, rice plants were cultivated hydroponically and then subjected to MeHg exposure, as shown in Supplementary Table 3. After exposure, rice plants were harvested, washed and analyzed for THg and MeHg concentrations. All the solutions were collected, weighed, and acidified before Hg analyses. The axenically cultured rice/callus (2 weeks, Rice-1, cultivated in Prof. Sihai Yang's lab, Nanjing University) were also used to quantify demethylation after being exposed to dissolved MeHg.

For *in vitro* tests, the roots of 1-month-old rice seedlings were homogenized in phosphate buffer in ice bath. Roots instead of the whole plant/shoots were used since roots are more capable of MeHg demethylation. These homogenates were then spiked with MeHg to a level of 100 μg/L and incubated at room temperature for 5 days. In order to evaluate the roles of rhizospheric and/or endophytic bacteria in MeHg demethylation (such as endophytes) [48], antibiotics (1% penicillin-streptomycin solution, v/v; GE Healthcare Life Sciences) were added to the homogenate. The demethylation in the supernatant fraction of homogenate (filtered by 0.22-μm membrane to exclude microorganisms, ASTM F838-05) was also explored. After incubation, all homogenates were analyzed for MeHg concentrations. The microbial community in homogenates (with or without antibiotics) was analyzed before and after incubation (16s rRNA, Sangon Biotech (Shanghai) Co., Ltd.).

Additionally, the role of culturable microorganisms isolated from roots in MeHg demethylation was also investigated. Briefly, fresh roots of Rice 1 (1-month-old) were surface sterilized [49], washed with sterilized DI water 7 times and homogenized, and then

the homogenates were inoculated into Luria Bertani (LB, for the cultivation of bacteria) or Potato Dextrose Agar (PDA, culture medium for fungi) solid medium. Three replicates were set for either bacteria or fungi. After inoculation, the plates with endophytic bacteria were cultivated at 37 ℃, while the endophytic fungi were cultivated at 28 ℃. After 10 days of cultivation, 2.5 mL of sterilized PBS (pH = 7.2) was added to each plate to wash the colonies. Then the PBS containing endophytes was transferred to sterilized centrifuge tubes. After mixing thoroughly, the optical densities (OD600, Infinite 200 pro, TECAN) of the PBS solutions were measured to determine the growth of endophytes. Next, OD600s of all the PBS containing endophytic bacteria or fungi were adjusted to 0.5 using PBS. A volume of 500 μL bacterial/fungal solution was then mixed with 500 μL sterilized LB/PDA, spiked with MeHg (10 μg/L) and then cultivated at 25 ℃ in the dark to quantify possible MeHg demethylation. After 5 days of cultivation, samples were collected to analyze the remaining MeHg. Meanwhile, the demethylation capacity of LB or PDA medium was also quantified. Specifically, 500 μL of cultivation medium was mixed with 500 μL PBS solution (20 mM). Then MeHg was spiked into each replicate to a final concentration of 10 μg/L and the mixtures were incubated as described above. After 5 days of incubation, samples were collected to analyze the remaining MeHg.

Hg release experiment. To identify the Hg species after MeHg demethylation, rice plants (Rice-1) were exposed to dissolved MeHg in a closed system (Extended Data Fig. 4). Specifically, two treatments, i.e., control (0.01 M $CaCl_2$ solution) and exposure treatment (ET, ~0.4 μg/L MeHg in 0.01 M $CaCl_2$ solution) were designed. Each treatment contained 3 replicates and each replicate contained 5 rice seedlings. The bottle with the exposure medium was sealed with Parafilm to prevent the contact of solution with the chamber. The chamber and the bottle holding the exposure medium were connected and sealed with Parafilm and tape. Compressed air, with residual Hg removed using a gold trap, was introduced into the chamber at a flow of ~30−50 mL/min. The air exiting the chamber was introduced to a gold trap (filled with gold-coated quartz) for Hg^0 collection or a Tenax-TA trap column (filled with Tenax-TA, an adsorbent for organic Hg) to collect Hg^0 and organic Hg species. After 80 h of exposure,

the chamber was separated from the bottle holding the uptake medium and capped immediately, ventilated for 30 min and washed with 5% BrCl solution. All the seedlings were washed (with shoots and roots separated) and dried as described above. All the solutions were acidified with HCl for THg and MeHg analyses. The recovery rate of Hg was monitored and found to be satisfactory (107%, details in Supplementary Table 9) for this closed system. To identify the source of the trapped Hg, this experiment was repeated (ET only) with the application of enriched $Me^{199}Hg$. The content of captured Hg^0 was analyzed using ICPMS.

Quencher addition experiments. To explore the potential roles of ROS in MeHg demethylation in plants, we quantified MeHg demethylation in response to quencher addition in root homogenates (obtained in ice bath) of 1-, 2- and 4-month-old rice plants. Specifically, β-carotene (10 mM, > 96%, Aladdin, China), tetrahydrofuran (THF, 50 mM, 99.5%, J&K, China) and dimethylfuran (DMFR, 50 mM, >99%, Damas-beta, China) were used to quench singlet oxygen, superoxide dismutase (SOD, 0.5 mg/L, derived from swine blood, Shanghai Yuanye Biotechnology Co., Ltd) was used to quench superoxide anion and isopropyl alcohol (ISP, 50 mM, > 99.9%, Aladdin, China) was used to quench hydroxyl radical [50]. Homogenates and PBS were added with quenchers and spiked with MeHg (100 μg/L). After being incubated for 5 days at 30 °C in the dark, homogenates were analyzed for MeHg contents.

Singlet oxygen-generating chemical system. To provide further evidence that singlet oxygen induces MeHg demethylation in the presence of thiols, we quantified demethylation in a singlet oxygen-generating chemical system, i.e., molybdate and H_2O_2. Specifically, 100 μL of molybdate and 50 μL of reduced glutathione (GSH) were added to PBS (900 μL) to a final concentration of 25 mM and 20 μM, respectively (refers to Singlet oxygen + GSH). Then 10 μL of MeHg standard solution (1 mg/L, Brooks Rand) was added and equilibrated for 1 h. PBS and treatment without GSH (Singlet oxygen treatment) were set as controls to quantify demethylation capacities of PBS buffer and singlet oxygen. The demethylation capacities of GSH, molybdate, and H_2O_2 alone were quantified and found to be negligible. After the equilibration, 10 μL of H_2O_2 (7.5%, w/v) was added to treatments of Singlet oxygen + GSH and Singlet

oxygen. The addition of H_2O_2 was repeated 5 times with a time interval of 40 min. Such an operation was designed to maintain a continuous generation of singlet oxygen. Thirty to forty min after the last addition, MeHg in each treatment, as well as MeHg in solutions before H_2O_2 addition, were detected for the calculation of the demethylation ratios.

2. Parameter analyses

Hg analysis. For isotopic THg, water samples were subjected to digestion with BrCl, while plant samples were digested by a mixture of HNO_3 and H_2SO_4 (7:3, v/v). $^{201}HgCl$ was added to all samples as an internal standard. After the reduction by $SnCl_2$, Hg was measured using inductively coupled plasma mass spectrometry (ICPMS) [51]. For isotopic MeHg analysis, both water and plant samples were distilled, ethylated and then measured using gas chromatography (GC)-ICPMS. $Me^{201}Hg$ was added to each sample as the internal standard. Analysis of duplication, matrix spikes and standard reference materials (for THg, lobster muscle, TORF-3, 290 ± 2.2 μg/kg; for MeHg, estuarine sediment, BCR-CRM 580, 75 ± 4 μg/kg) were included in each analytical session. Isotope dilution calculations and further details could be found in Hintelmann and Ogrinc [52]. It should be noted that due to the relatively low enrichment of spiked $I^{200}Hg$, the enrichments of other Hg isotopes were subtracted according to the proportions of each isotope (obtained from the manufacturer) during the calculation. The recoveries of standard reference material were 90−96% (n = 3) for THg and 91−107% (n = 4) for MeHg. The recoveries of matrix spike for water digestion (THg) were 88−109% and the relative standard deviations for duplicated distillation and analysis were < 10%.

For ambient THg analysis, samples were analyzed using an automated Hg analyzer (Brooks Rand, USA) after digestion with concentrated HNO_3 and H_2SO_4 (7:3, v/v). Analytical duplicates and standard reference material (citrus leaf, GBW10020, 150 ± 20 μg/kg) were applied to each batch of analysis and the recoveries of the standard reference material were 105 ± 10% (n = 16) for THg. The recoveries of matrix spike were 95 ± 7% (n = 12). For MeHg, plant samples were digested with 2 mL of 25% (w/w) KOH-CH_3OH at 60 °C for 4 h and then the concentrations were determined using

an automated MeHg analyzer (Brooks Rand, USA), based on EPA Method 1630. Matrix spike and standard reference material (BCR-CRM 580) recoveries ranged from 88−105%. The effects of various ROS quenchers on MeHg analyses were checked by standard addition, and the recoveries ranged from 91−105% (Supplementary Table 5).

Hg species in traps from the Hg release experiment were analyzed using manual Hg analysis systems. Specifically, for organic Hg analysis, the Tenax-TA trap columns were heated to 120 °C within 30 secs. All adsorbed Hg were released and separated through a GC column (15% OV3, 680 mm; temperature, 30 °C; Ar flow, 50 mL/min), pyrolyzed to elemental Hg and analyzed by atomic fluorescence spectroscopy (Brooks Rand). Due to the high toxicity of dimethylmercury (DMHg), the instrument response to MeHg standard was used to quantify DMHg. The GC peak between elemental Hg and MeHg is identified as DMHg. For elemental Hg analysis, gold trap columns were heated to 500 °C within 15 secs under a stream of Ar (50 mL/min). The Hg was then analyzed by atomic fluorescence spectroscopy. For the analysis of $^{199}Hg^0$, trapped Hg was desorbed at 500 °C and introduced into a $KMnO_4$ solution with flowing Ar, and then the solution was neutralized with hydroxylamine hydrochloride before the analysis using ICPMS.

Singlet oxygen analysis. Singlet oxygen from rice roots was detected using electron paramagnetic resonance (EPR, E500, Bruker). 2,2,6,6-Tetramethyl-4-piperidone hydrochloride (TEMPD-HCl, 500 mM, Dojindo, Japan, prepared with 20 mM phosphate buffer/D_2O, pH = 7) was used as the spin trap [53]. D_2O, instead of H_2O was used to prepare the phosphate buffer, considering that singlet oxygen has a longer lifetime in D_2O [54]. Roots of rice plants (1-, 2-, 3-, 4- and 5-month-old) were exposed to 2 mL of TEMPD-HCl for 1 h, after which the solution was subjected to the detection of singlet oxygen; meanwhile, the 20 mM phosphate buffer/D_2O was taken as the blank. EPR conditions were as follows: microwave frequency, 9.84 GHz; microwave power, 6.325 mW; field modulation frequency, 100 kHz; amplitude, 0.1 mT; sweep width, 200 G; sampling time, 40 s; and receiver gain, 42 dB.

Additionally, singlet oxygen in shoots and roots was imaged using singlet oxygen sensor green (SOSG, meilunbio, China) as the probe molecule [32]. Specifically, rice

plants at ages of 1-, 2-, or 4-month-old were completely immersed in a 50 μM SOSG solution and cultivated for 30 minutes in the dark, then rinsed with DI water three times and photographed with a fluorescence microscope (Zeiss Axio Imager. A, Germany). Singlet oxygen detection was conducted by recording the fluorescence emission spectra of SOSG (excitation/emission = 504/525 nm) with the excitation wavelength fixed at 488 nm.

3. Model estimation

This model was developed to evaluate the protective effects of rice-mediated demethylation on human health in non-Hg contaminated areas. This evaluation is essential, considering that 1) rice consumption is a major source of dietary MeHg exposure for Asians due to the high consumption rate of rice, e.g., accounting for up to 96% of MeHg exposure in China [21]. 2) Even low-level dietary exposure to MeHg during pregnancy negatively affects a newborn's lifelong intelligence quotient (IQ) [40]. It is also important to note that although photolysis and microbial demethylation may also contribute to reducing MeHg accumulation in rice, their potential contributions are excluded in model estimation. This is because the DRs used in the estimation are quantified under conditions with the interferences of both photolysis and microbial demethylation (Supplementary Text 7).

Cg_0. Cg_0 (μg/kg) is the estimated MeHg concentration in rice grains without *in vivo* demethylation and is calculated based on the observed demethylation ratios (DRs, defined as the ratio of demethylated MeHg to total absorbed MeHg by rice plants). To calculate Cg_0, we first assume that the amount of MeHg accumulated by 1 ha of rice plants per day is Am (mg MeHg/ha/d). Therefore, the whole rice plants accumulate 150 Am mg MeHg/ha for the entire growth period, assuming the net MeHg accumulation in rice plants increases linearly over the 5 months of growth [55]. Thus, DR on day *i* (DR_i) is calculated as:

$$DR_i = (Ab_i\text{-}Am)/Ab_i \text{------(1)}$$

Where Ab_i is the amount of MeHg absorbed in rice plants for 1 ha on day *i*. Therefore, Ab_i could be estimated as:

$Ab_i = Am/(1-DR_i)$ ------(2)

For DR_i, we quantified DRs on the 30th, 90th and 150th day of rice growth, i.e., 70.51%, 63.23% and 32.71% for DR_{30}, DR_{90} and DR_{150}, respectively. For DR_i ($i > 30$), we assume that DR changes linearly between two adjacent time points, and the DR_i could be therefore calculated by linear interpolation between the observed DRs. While for DRs during the first month (i.e., $i < 30$), we calculate these under 2 scenarios between DR_0 to DR_{30}: A, DR increases linearly from 0 to 70.51% and B, DR decreases linearly from 100 to 70.51%. Due to the lack of DR data through rice growth stages for other varieties, we only applied the DRs quantified from Rice 1 to the estimations of DR_i. It should be noted that although the quantified DRs are comparable among different rice varieties (Fig. 1h) and different MeHg exposure concentrations (Extended Data Fig. 3a), other environmental factors may impact MeHg uptake and, thus, DRs, leading to uncertainties in this estimation.

For Am, it is calculated according to the following equation:

$Am = Cg \times Yd/p/1000/150$ ------(3)

Where Cg represents the MeHg levels determined in rice grains (μg/kg), which are retrieved from published papers (Supplementary Table 6). It should be noted that we aimed to estimate the rice MeHg in non-Hg contaminated areas, and thus any rice MeHg concentration data obtained from Hg-contaminated areas are excluded. Yd is the rice yield (kg/ha); p refers to the ratio of the amount of MeHg in rice grains (ng) to that in the whole plant (ng); 1000 is the coefficient to convert μg to mg and 150 is the duration of rice plant growth (d).

Therefore, the Cg_0 (μg/kg) is calculated as:

$Cg_0 = Sum\ (Ab_1: Ab_{150}) \times p/Yd$ ------(4)

IQ decrement. Methylmercury has adverse effects on infant cognition, resulting in intelligence quotient (IQ) deficits. Previous epidemiological studies have shown that there is a linear dose-response relationship between maternal intake of MeHg and fetal IQ decrements [38,39]. Based on that, the coefficients of MeHg from dietary intake to blood MeHg level (β, μg Hg/L blood per μg Hg/d), blood MeHg level to hair MeHg level (λ, μg Hg/g hair per μg Hg/blood) and maternal hair MeHg to infant IQ (γ, IQ point per μg

592 Hg/g hair) are applied to estimate IQ decrements [3,56] and the avoided IQ decrement
593 (ΔIQ) is calculated as:

594 $$\Delta IQ = \beta \times \lambda \times \gamma \times IR \times (Cg_0 - Cg) \text{ ------(5)}$$

595 Where IR is the rice consumption rate (kg/capita/d), which is obtained from the
596 FAO website (http://www.fao.org/faostat/en/#data/CC); Cg_0 is the MeHg level in rice
597 grains without MeHg demethylation and Cg is the observed MeHg level in rice grains
598 (μg/kg). Cg data are obtained from the published literatures, and any data from Hg
599 contaminated areas or Hg-spiking/soil-amending experiments are excluded. Rice trade
600 was not considered here, because 1) in major rice planting countries (listed in
601 Supplementary Table), residents mainly consume domestic rice as rice import
602 accounted for less than 10% of the total production (data in 2015, FAO), and 2) for the
603 other countries, we used the average MeHg concentration of the data obtained from
604 major rice planting countries. For β and λ, 0.763 and 0.365 are adopted in this study
605 (details in below), considering that these values are higher in the rice-diet [57] than those
606 in the fish-diet (normally 0.6 and 0.21 are used). For the value of γ, 0.3 is used [3]. Details
607 of these parameters are listed in Supplementary Table 6.

608 **β** The coefficient of rice intake to blood (μg Hg/L blood per μg Hg/day) is
609 calculated as:

610 $$\beta = fa \times fb/(t \times V) \text{------(6)}$$

611 Where fa and fb are the absorption rates of MeHg by gut and in blood; generally,
612 95% and 5% are adopted for fa and fb [58]. t is the elimination rate (0.014/day) and V is
613 the blood volume (L, 8% of body weight, bw). Therefore, equation 1 can be simplified
614 as:

615 $$\beta = 42.417/bw \text{------(7)}$$

616 Li et al. carried out a study in a Hg mining impacted area [57]. They collected rice,
617 blood, and hair samples, and obtained information on body weight, age, gender and rice
618 intake rate via questionnaire. Thus, the β value could be calculated according to the
619 obtained body weights.

Economic benefits. It is believed that IQ decrements in infants lead to lower cognitive performance and academic achievement, causing long-term impacts on lifetime earnings. Previous studies have estimated the effects of IQ decrements on hourly wages for males and females [42,43], while we use a weight-averaged rate for both genders since delineating differences between genders is not the aim of this study. The weight averaged rate has also been commonly applied to other studies [4,59]. IQ deficits have direct and indirect effects on lifetime earnings [42], and the percentage of lifetime earnings per IQ point loss ranges from 1.76% to 2.37%, as suggested by Grosse et al. [60]. We also use the purchasing power parity (PPP) adjusted GDP as the lifetime earnings for 159 countries/regions [4] since data are available for these areas. A 30-year (from 1986−2015) averaged GDP growth rate is used as lifetime earnings growth rate. The PPP adjusted GDP, together with the growth rate of lifetime earnings and years of working (35 years), are applied to estimate the lifetime earnings (LE), and thus the economic benefits (EB) generated from avoided IQ decrement could be calculated as:

$$EB = LE \times r \times \Delta IQ \times IB \quad (8)$$

Where r is the proportion of the economic loss per IQ loss to earnings coefficient (%), and the values of LE in different countries are estimated based on the average earnings [3]. IB represents the number of new births in a year. More details about the parameters are presented in Supplementary Table 6.

It should be noted that the estimations of Cg_0, IQ decrement, and economic benefits are not focus on Hg-contaminated areas. It is because the observed demethylation occurs in rice plants irrespective of MeHg exposure concentration, and all the data used in the estimations were obtained from non-contaminated areas.

Uncertainty analysis. Monte Carlo simulation (MCS) is used to estimate the uncertainty of avoided IQ decrement (ΔIQ) and economic benefits (EB).

As for ΔIQ in both scenarios, after integrating related equations, they are functions of Cg, β, λ, γ and IR, as shown below:

$$\text{In Scenario A, } \Delta IQ = \beta \times \lambda \times \gamma \times IR \times 1.4 \times Cg \quad (9)$$

$$\text{In Scenario B, } \Delta IQ = \beta \times \lambda \times \gamma \times IR \times 3.7 \times Cg \quad (10)$$

649 Where 1.4 and 3.7 are coefficients for the increases in rice MeHg concentrations
650 under the two scenarios. Details about these parameters, including the mean value,
651 standard deviation, the minimum and the maximum values, are presented in
652 Supplementary Table 6 and Source Data.
653 The calculation of EB in Scenarios A and B can be simplified as follows:
654 In Scenario A, $EB = \beta \times \lambda \times \gamma \times IR \times 1.4 \times Cg \times LE \times r \times IB$------ (11)
655 In Scenario B, $EB = \beta \times \lambda \times \gamma \times IR \times 3.7 \times Cg \times LE \times r \times IB$ ------ (12)
656 All the inputs for the uncertainty analysis of ΔIQ are listed in Supplementary Table
657 7. A total of 100,000 iterations are needed to achieve the stabilization of the percentiles
658 with deviations of less than 5%. Runs are made using Microsoft Excel (Microsoft
659 Corporation, Microsoft Office Home and Student 2019).

660 **4. Estimation of Hg release via MeHg or IHg uptake**

661 To compare the gaseous Hg released from rice plants following root uptake of
662 MeHg and IHg, we firstly applied the Hg release data from the enriched isotope
663 experiment to calculate Hg release capacity following MeHg or IHg exposure. The
664 capacity of Hg release is expressed as ng released Hg per μg/L exposed Hg.
665 Specifically, the total mass of $T^{202}Hg$ in whole plants decreased from 32.76 ng at T1 (0
666 h after exposure) to 7.13 ng at T3 (72 h after exposure), with a net decrease of 25.63
667 ng. Considering that the exposure concentration was 0.4 μg MeHg/L, the capacity of
668 Hg release is calculated as 64.08 ng Hg per μg/L MeHg. Similarly, the capacity of Hg
669 release via IHg uptake is calculated based on the decrease in $T^{200}Hg$ (i.e., 0.062 ng from
670 T1 to T3). Given that the exposure concentration of $I^{200}Hg$ was 0.15 μg/L, the capacity
671 is estimated as 0.42 ng Hg per μg/L IHg. Thus, the capacity of Hg release following
672 MeHg uptake is ~153 times higher than that following IHg uptake at the same exposure
673 concentration. This, together with the documented ratios of MeHg to IHg in sediment
674 pore water (Supplementary Table 8), are then used to estimate the relative contribution
675 of MeHg and IHg in pore water to Hg release from rice. By multiplying 1) the average
676 ratio of MeHg to IHg in pore water (0.19, Supplementary Table 8) and 2) the ratio of

Hg release capacity of MeHg to IHg (i.e., 153), we estimate that the average contribution via MeHg uptake is ~30 times higher than that via IHg uptake.

5. Density-functional theory calculations

Density-functional theory (DFT) calculations are carried out using the Gaussian 16 suite of programs [61], with meta-hybrid M06 functional [62] to investigate Hg-C bond cleavage in MeHg by singlet oxygen in the presence or absence of thiol (glutathione/GSH). The 6-311+G(d,p) basis set (or 6-311+G(d,p)//6-31G(d) for system containing GSH) is used in geometry optimizations for all elements except Hg, for which ECP60MWB basis set is used to incorporate the Wood-Boring quasi-relativistic effective core potential (ECP) [63]. The spin contamination error of the system containing singlet oxygen is eliminated using the broken-symmetry solution by mixing HOMO and LUMO orbitals. Vibration analyses are performed for all complexes and transition structures to obtain zero-point energies and to confirm transition states. The solvent effect is computed in all calculations using the continuum solvation model density (SMD) [64].

References

1. UNEP. *Global Mercury assessment 2018*. (2018).
2. Karagas, M. R. *et al.* Evidence on the human health effects of low-level methylmercury exposure. *Environ Health Perspect* **120**, 799–806 (2012).
3. Rice, G. E., Hammitt, J. K. & Evans, J. S. A probabilistic characterization of the health benefits of reducing methyl mercury intake in the United States. *Environ Sci Technol* **44**, 5216–5224 (2010).
4. Bellanger, M. *et al.* Economic benefits of methylmercury exposure control in Europe: Monetary value of neurotoxicity prevention. *Environ Health* **12**, 1–10 (2013).
5. Grandjean, P., Pichery, C., Bellanger, M. & Budtz-Jørgensen, E. Calculation of Mercury's effects on Neurodevelopment. *Environ Health Perspect* **120**, 452 (2012).
6. Zhang, Y. *et al.* Global health effects of future atmospheric mercury emissions. *Nat Commun* **12**, 3035 (2021).
7. Chen, L. *et al.* Trans-provincial health impacts of atmospheric mercury emissions in China. *Nat Commun* **10**, 1484 (2019).
8. Seller, P., Kelly, C. A., Rudd, J. W. M. & Mac Hutchon, A. R. Photodegradation of methylmercury in lakes. *Nature* **380**, 694–697 (1996).
9. Klapstein, S. J., Ziegler, S. E., Risk, D. A. & O'Driscoll, N. J. Quantifying the effects of photoreactive dissolved organic matter on methylmercury photodemethylation rates in freshwaters. *Environ Toxicol Chem* **36**, 1493–1502 (2017).

10. Kronberg, R. M., Schaefer, J. K., Björn, E. & Skyllberg, U. Mechanisms of Methyl Mercury Net Degradation in Alder Swamps: The Role of Methanogens and Abiotic Processes. *Environ Sci Technol Lett* **5**, 220–225 (2018).
11. Zhou, X. Q. *et al.* Microbial Communities Associated with Methylmercury Degradation in Paddy Soils. *Environ Sci Technol* **54**, 7952–7960 (2020).
12. Wu, Q. *et al.* Methanogenesis Is an Important Process in Controlling MeHg Concentration in Rice Paddy Soils Affected by Mining Activities. *Environ Sci Technol* **54**, 13517–13526 (2020).
13. Barkay, T. & Gu, B. Demethylation-The Other Side of the Mercury Methylation Coin: A Critical Review. *ACS Environmental Au* **2**, 77–97 (2022).
14. Feyte, S., Gobeil, C., Tessier, A. & Cossa, D. Mercury dynamics in lake sediments. *Geochim Cosmochim Ac* **82**, 92–112 (2012).
15. Hammerschmidt, C. R. & Fitzgerald, W. F. Photodecomposition of methylmercury in an arctic Alaskan lake. *Environ Sci Technol* **40**, 1212–1216 (2006).
16. Lehnherr, I., St. Louis, V. L., Emmerton, C. A., Barker, J. D. & Kirk, J. L. Methylmercury cycling in high arctic wetland ponds: Sources and sinks. *Environ Sci Technol* **46**, 10514–10522 (2012).
17. Xu, X. *et al.* Demethylation of methylmercury in growing rice plants: An evidence of self-detoxification. *Environ Pollut* **210**, 113–120 (2016).
18. Li, Y. *et al.* The influence of iron plaque on the absorption, translocation and transformation of mercury in rice (Oryza sativa L.) seedlings exposed to different mercury species. *Plant Soil* **398**, 87–97 (2016).
19. Strickman, R. J. & Mitchell, C. P. J. Accumulation and translocation of methylmercury and inorganic mercury in Oryza sativa: An enriched isotope tracer study. *Sci Total Environ* **574**, 1415–1423 (2017).
20. Liu, M. *et al.* Rice life cycle-based global mercury biotransport and human methylmercury exposure. *Nat Commun* **10**, 5164 (2019).
21. Gong, Y. *et al.* Bioaccessibility-corrected risk assessment of urban dietary methylmercury exposure via fish and rice consumption in China. *Sci Total Environ* **630**, 222–230 (2018).
22. Cui, W. *et al.* Occurrence of Methylmercury in Rice-Based Infant Cereals and Estimation of Daily Dietary Intake of Methylmercury for Infants. *J Agric Food Chem* **65**, 9569–9578 (2017).
23. Zhu, W. *et al.* Global observations and modeling of atmosphere-surface exchange of elemental mercury: A critical review. *Atmos Chem Phys* **16**, 4451–4480 (2016).
24. Hsu-Kim, H., Kucharzyk, K. H., Zhang, T. & Deshusses, M. A. Mechanisms regulating mercury bioavailability for methylating microorganisms in the aquatic environment: A critical review. *Environ Sci Technol* **47**, 2441–2456 (2013).
25. Bishop, K. *et al.* Recent advances in understanding and measurement of mercury in the environment: Terrestrial Hg cycling. *Sci Total Environ* **721**, 137647 (2020).
26. Zhou, J., Obrist, D., Dastoor, A., Jiskra, M. & Ryjkov, A. Vegetation uptake of mercury and impacts on global cycling. *Nat Rev Earth Environ* **2**, 269–284 (2021).
27. Obrist, D. *et al.* A review of global environmental mercury processes in response to human and natural perturbations: Changes of emissions, climate, and land use. *Ambio* **47**, 116–140 (2018).
28. Zhang, T. & Hsu-Kim, H. Photolytic degradation of methylmercury enhanced by binding to natural organic ligands. *Nat Geosci* **3**, 473–476 (2010).

29. Luo, H., Cheng, Q. & Pan, X. Photochemical behaviors of mercury (Hg) species in aquatic systems: A systematic review on reaction process, mechanism, and influencing factor. *Sci Total Environ* **720**, 137540 (2020).
30. Gill, S. S. & Tuteja, N. Reactive oxygen species and antioxidant machinery in abiotic stress tolerance in crop plants. *Plant Physiol Biochem* **48**, 909–930 (2010).
31. Chen, T. & Fluhr, R. Singlet oxygen plays an essential role in the root's response to osmotic stress. *Plant Physiol* **177**, 1717–1727 (2018).
32. Koh, E., Carmieli, R., Mor, A. & Fluhr, R. Singlet oxygen-induced membrane disruption and serpin-protease balance in vacuolar-driven cell death. *Plant Physiol* **171**, 1616–1625 (2016).
33. Taverne, Y. J. *et al.* Reactive Oxygen Species: Radical Factors in the Evolution of Animal Life: A molecular timescale from Earth's earliest history to the rise of complex life. *BioEssays* **40**, 1–9 (2018).
34. Sheng, F. *et al.* A new pathway of monomethylmercury photodegradation mediated by singlet oxygen on the interface of sediment soil and water. *Environ Pollut* **248**, 667–675 (2019).
35. Shapiro, A. M. & Chan, H. M. Characterization of demethylation of methylmercury in cultured astrocytes. *Chemosphere* **74**, 112–118 (2008).
36. Yasutake, A. & Hirayama, K. Evaluation of methylmercury biotransformation using rat liver slices. *Arch Toxicol* **75**, 400–406 (2001).
37. Suda, I., Totoki, S. & Takahashi, H. Degradation of methyl and ethyl mercury into inorganic mercury by oxygen free radical-producing systems: involvement of hydroxyl radical. *Arch Toxicol* **65**, 129–134 (1991).
38. Crump, K. S., Kjellström, T., Shipp, A. M., Silvers, A. & Stewart, A. Influence of prenatal mercury exposure upon scholastic and psychological test performance: Benchmark analysis of a New Zealand cohort. *Risk Analysis* **18**, 701–713 (1998).
39. Grandjean, P. *et al.* Cognitive deficit in 7-year-old children with prenatal exposure to methylmercury. *Neurotoxicol Teratol* **19**, 417–428 (1997).
40. Myers, G. J. *et al.* Prenatal methylmercury exposure from ocean fish consumption in the Seychelles child development study. *Lancet* **361**, 1686–1692 (2003).
41. Rothenberg, S. E. *et al.* Stable Mercury Isotopes in Polished Rice (Oryza sativa L.) and Hair from Rice Consumers. *Environ Sci Technol* **51**, 6480–6488 (2017).
42. Salkever, D. S. Updated estimates of earnings benefits from reduced exposure of children to environmental lead. *Environmental Research* **70** 1–6 (1995).
43. Heckman, J. J., Stixrud, J. & Urzua, S. The effects of cognitive and noncognitive abilities on labor market outcomes and social behavior. *J Labor Econ* **24**, (2006).
44. Zhang, W. *et al.* Economic evaluation of health benefits of mercury emission controls for China and the neighboring countries in East Asia. *Energy Policy* **106**, 579–587 (2017).
45. Hasanuzzaman, M. *et al.* Reactive Oxygen Species and Antioxidant Defense in Plants under Abiotic Stress: Revisiting the Crucial Role of a Universal Defense Regulator. *Antioxidants* **2020**, 681.
46. Rothenberg, S. E. & Feng, X. Mercury cycling in a flooded rice paddy. *J Geophys Res Biogeosci* **117**, (2012).
47. Tang, W. *et al.* Increased Methylmercury Accumulation in Rice after Straw Amendment. *Environ Sci Technol* **53**, 6144–6153 (2019).

48. Lee, C. S. & Fisher, N. S. Microbial generation of elemental mercury from dissolved methylmercury in seawater. *Limnol Oceanogr* **64**, 679–693 (2019).
49. Mence Chaintreuil, C. *et al.* Photosynthetic Bradyrhizobia Are Natural Endophytes of the African Wild Rice *Oryza breviligulata*. *Applied Environ Microbial* 66, 5437–5447 (2000).
50. Han, X., Li, Y., Li, D. & Liu, C. Role of Free Radicals/Reactive Oxygen Species in MeHg Photodegradation: Importance of Utilizing Appropriate Scavengers. *Environ Sci Technol* **51**, 3784–3793 (2017).
51. Štrok, M., Hintelmann, H. & Dimock, B. Development of pre-concentration procedure for the determination of Hg isotope ratios in seawater samples. *Anal Chim Acta* **851**, 57–63 (2014).
52. Hintelmann, H. & Ogrinc, N. Determination of stable mercury isotopes by ICP/MS and their application in environmental studies. in *Biogeochemistry of Environmentally Important Trace Elements* 321–338 (2003).
53. Krieger-Liszkay, A., Trösch, M. & Krupinska, K. Generation of reactive oxygen species in thylakoids from senescing flag leaves of the barley varieties Lomerit and Carina. *Planta* **241**, 1497–1508 (2015).
54. Ossola, R., Jönsson, O. M., Moor, K. & McNeill, K. Singlet Oxygen Quantum Yields in Environmental Waters. *Chem Rev* 121, 4100–4146 (2021).
55. Meng, B. *et al.* The Process of Methylmercury Accumulation in Rice (Oryza sativa L.). *Environ Sci Technol* **45**, 2711–2717 (2011).
56. Giang, A. & Selin, N. E. Benefits of mercury controls for the United States. *Proc Natl Acad Sci U S A* **113**, 286–291 (2016).
57. Li, P., Feng, X., Chan, H. M., Zhang, X. & Du, B. Human body burden and dietary methylmercury intake: The relationship in a rice-consuming population. *Environ Sci Technol* **49**, 9682–9689 (2015).
58. U.S. Environmental Protection Agency. *Mercury Study Report to Congress Volume V: Health Effects of Mercury and Mercury Compounds*. (1997).
59. Gould, E. Childhood lead poisoning: Conservative estimates of the social and economic benefits of lead hazard control. *Environ Health Perspect* **117**, 1162–1167 (2009).
60. Grosse, S. D., Matte, T. D., Schwartz, J. & Jackson, R. J. Economic gains resulting from the reduction in children's exposure to lead in the United States. *Environ Health Perspect* **110**, 563–569 (2002).
61. Frisch, M. J. *et al.* Gaussian 16. Preprint at (2016).
62. Zhao, Y. & Truhlar, D. G. The M06 suite of density functionals for main group thermochemistry, thermochemical kinetics, noncovalent interactions, excited states, and transition elements: Two new functionals and systematic testing of four M06-class functionals and 12 other functionals. *Theor Chem Acc* **120**, 215–241 (2008).
63. Andrae, D., Iubermann, U. H., Dolg, M., Stoll, H. & Preub, H. Theoretica Chimica Acta Energy-adjusted ab initio pseudopotentials for the second and third row transition elements. *Theor Chim Acta* **77**, 123–141 (1990).
64. Marenich, A. v., Cramer, C. J. & Truhlar, D. G. Universal solvation model based on solute electron density and on a continuum model of the solvent defined by the bulk dielectric constant and atomic surface tensions. *J Physical Chem B* **113**, 6378–6396 (2009).

Acknowledgements

The authors gratefully acknowledge Dr. Lijun Gan from Nanjing Agriculture University for the advices on endophytes. W.T. appreciates the financial supports from National Natural Science Foundation of China (42107223), Fundamental Research Funds for the Central Universities (021114380175) and Natural Science Foundation of Jiangsu Province (BK20190319). Y.G. is supported by National Natural Science Foundation of China (U2032201). J.Z thanks the support from National Natural Science Foundation of China (12222509). H.H. acknowledges the funding from the NSERC Discovery Grant Program (RGPIN-2018-05421). S.L. appreciates Golden Goose Research Grant Scheme (GGRG) (UMT/RMIC/2-2/25 Jld 5 (64), Vot 55191). A.J. and B.G. are supported by the Office of Biological and Environmental Research within the Office of Science of the U.S. Department of Energy (DOE) at Oak Ridge National Laboratory, which is managed by UT-Battelle, LLC under Contract No. DE-AC05-00OR22725 with DOE.

Author Contributions

H.Z., J.Z. and Y.G. led this project and designed all experiments. W.T. carried out the enriched isotope experiment under the supervision of H.H.. W.T., X.B., Y.Z., Y.Y., J.W., and S.L. conducted the crop experiment, rice growth stage experiment, Hg release experiment, homogenate experiment and quencher addition experiment under the supervisions of J.Z., Y.G. and H.Z.. W.T. estimated the avoided IQ decrements/economic benefits and Hg releases, L.N. helped conduct the sensitivity analysis, and C.L. conducted density-functional theory calculations. W.T., H.Z. and C.S. led the manuscript writing and revision, and all coauthors participated in the writing and/or editing.

Competing interest declaration

The authors declare no competing interests.

Additional information

Supplementary Information is available for this paper and includes Supplementary Text, Supplementary Tables and Supplementary References.

Extended Data Figures

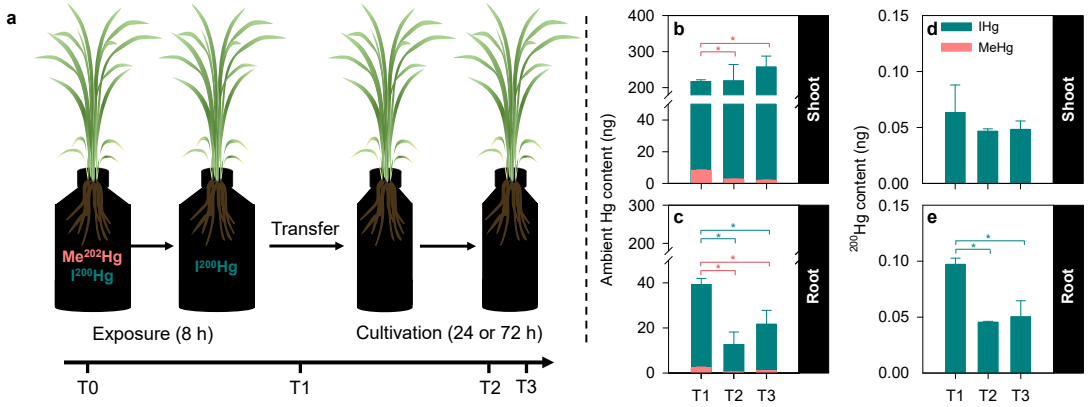

Extended Data Fig. 1 The design of the enriched isotope experiment (a), and the contents of ambient Hg (b and c) and ^{200}Hg (d and e) in rice tissues. T0 refers to the time when exposure started (Me^{202}Hg and I^{200}Hg spiked into solutions); T1 refers to the time when exposure ended and plants were transferred (Only significant proportion of I^{200}Hg remained in the solution, Supplementary Text 3); T2 and T3 refer to times when plants were further cultivated in Hg-free solution for 24 h (T2) and 72 h (T3), respectively. The contents of both THg and MeHg are calculated as the total mass (ng) to exclude the effect of biomass variability on concentration (i.e., biodilution). For panels (b) to (e), data are shown as mean ± SD, n = 3. Asterisk (*) indicates significant ($p < 0.05$) differences between two time points.

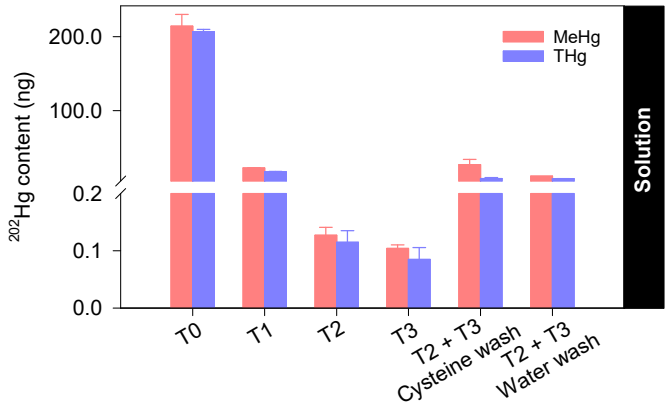

881

882 **Extended Data Fig. 2 Contents of T^{202}Hg and Me^{202}Hg in solutions of the enriched**
883 **isotope experiment.** T0 refers to the time when exposure started; T1 refers to the time when
884 exposure ended and plants were transferred; T2 and T3 refer to times when plants were further cultivated
885 in Hg-free solution for 24 h (T2) and 72 h (T3), respectively. Hg in cysteine wash and water wash
886 includes the washing solutions for both roots and shoots. The contents of both THg and MeHg are
887 calculated as the total mass (ng) in solution. Mean ± SD, n = 3.

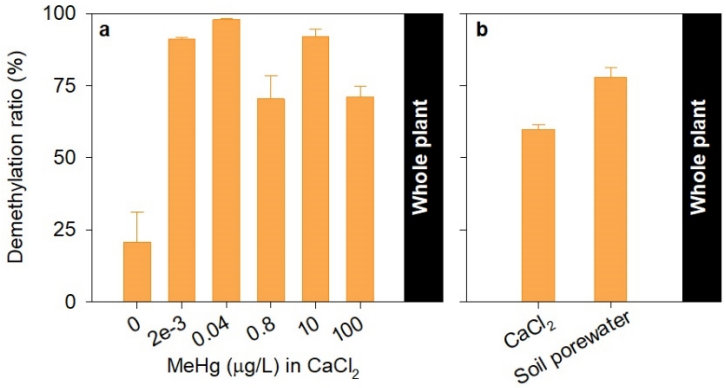

888

889 **Extended Data Fig. 3 The demethylation ratios (DRs) in rice plants after exposure**
890 **to different concentrations of MeHg (a) and to 0.8 μg/L MeHg in different matrices**
891 **(b).** Note that experiments for panels (a) and (b) were conducted separately and thus the slightly lower
892 DR in plants treated with $CaCl_2$ solution (b) compared with that in panel (a) is likely due to differences
893 in the growth condition. Mean ± SD, n = 3. Noted that in panel a, DR at concentration of 0 was quantified
894 separately and 4 replicates were set.

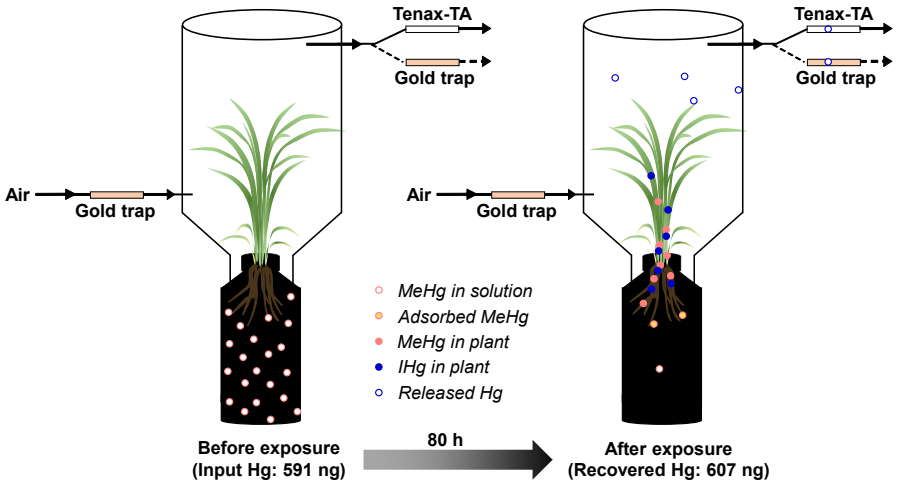

Extended Data Fig. 4 Experimental design and Hg distribution after 80-h exposure in the Hg release experiment. It should be noted that this is a conceptual scheme, and details about Hg proportions and the recovery rate can be found in Supplementary Table 9.

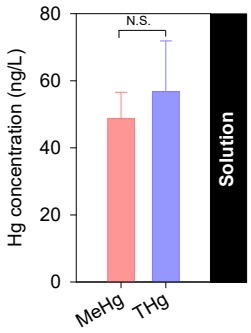

Extended Data Fig. 5 The concentrations of MeHg and THg in solution after exposure in the Hg release experiment. N.S. indicates no significant difference between two parameters ($p > 0.05$). Mean ± SD, n = 3.

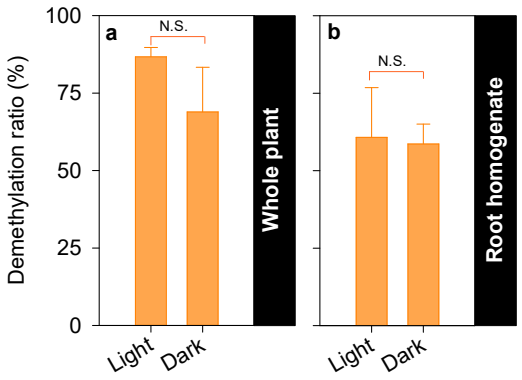

904

905 **Extended Data Fig. 6 The effect of light on MeHg demethylation *in vivo* (a) and *in**

906 ***vitro* (b).** N.S. indicates no significant difference between two treatments ($p > 0.05$). Mean ± SD, n =

907 3.

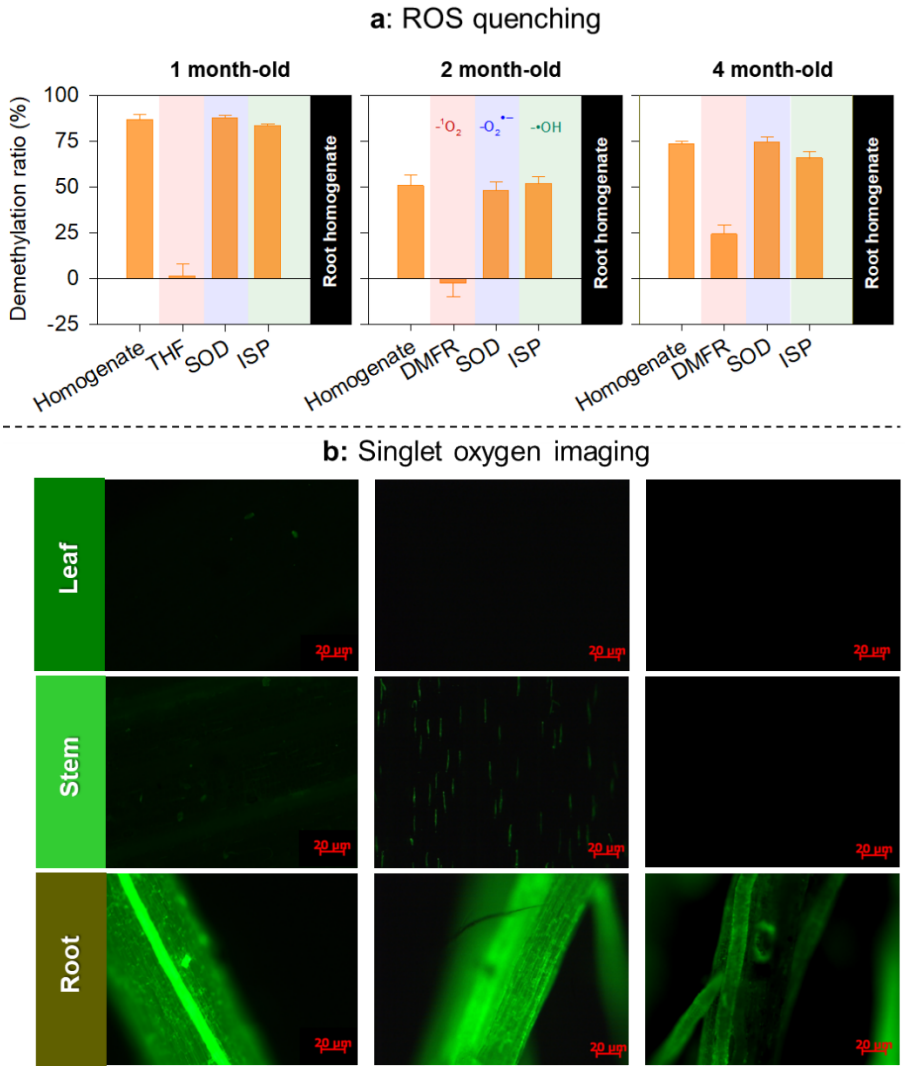

Extended Data Fig. 7 The response of MeHg demethylation in root homogenates of rice plants to radical quencher additions (a) and the appearance of singlet oxygen from rice plants (1-, 2- and 4-month-old, left to right in panel b) using SOSG. THF instead of DMFR was used in 1-month-old plants to scavenge singlet oxygen since the type of quencher has only a minor effect on the DR. In panel (a), data are shown as mean ± SD, n = 3.

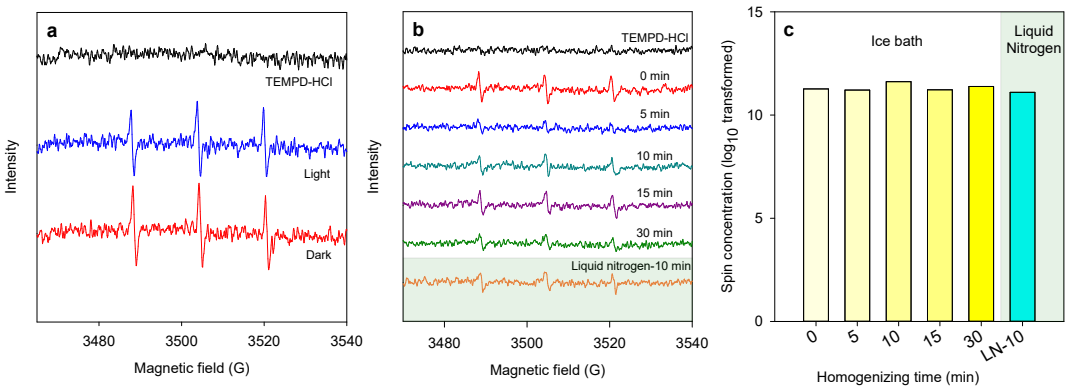

914

915 **Extended Data Fig. 8 The EPR signal of singlet oxygen in supernatant fraction (<**
916 **0.22 μm) under the light or dark condition (a), and its signal (b) and spin**
917 **concentrations in homogenates with different degrees of homogenization (c).**

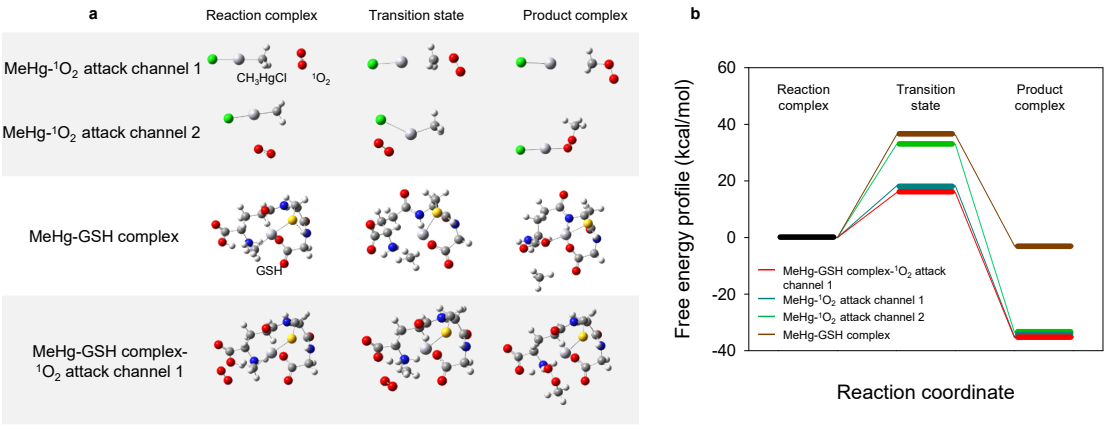

Extended Data Fig. 9 The optimized geometries for the reactants, transition states and products for reactions of Hg-C bond cleavage in MeHg by the attack of singlet oxygen, or Hg-C bond cleavage in MeHg-GSH in the presence/absence of the attack of singlet oxygen (a) and Gibbs free-energy profiles of Hg-C bond cleavages in all reaction systems (b).

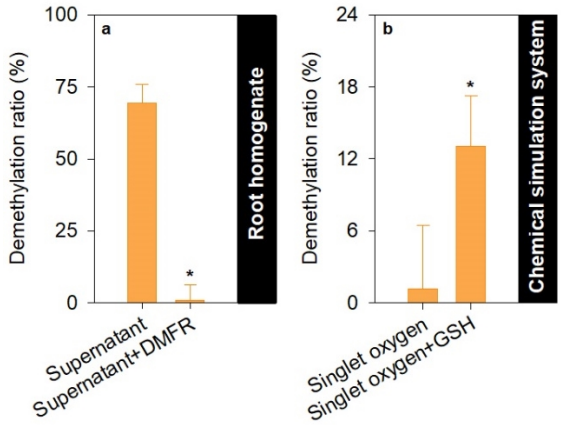

923

924 **Extended Data Fig. 10 The demethylation ratio of MeHg in the supernatant of root homogenate (<**
925 **0.22 μm fraction) without or with singlet oxygen quenched (a) and in singlet oxygen-generating**
926 **chemical system in the absence or presence of GSH (b).** In (a), data are presented as mean ± SD, n =
927 3. In (b), this experiment was repeated 3 times, and 3 replicates were set each time; thus, data are depicted
928 as mean ± SD, n = 9.